Reactive Transport Modelling of Dissolved CO2 Injection in a Geothermal Doublet. Application to the CO2 -DISSOLVED Concept

Christelle Castillo, Nicolas C.M. Marty, Virginie Hamm, Christophe Kervévan, Dominique Thiéry, Louis de Lary de Latour, Jean-Charles Manceau

Available online at www.sciencedirect.com

ScienceDirect

Energy Procedia 114 (2017) 4062 – 4074

Energy Procedia

13th International Conference on Greenhouse Gas Control Technologies, GHGT-13, 14-18 November 2016, Lausanne, Switzerland

Reactive transport modelling of dissolved CO_2 injection in a geothermal doublet. Application to the CO_2-DISSOLVED concept

Christelle Castillo[a], Nicolas C.M. Marty[a]*, Virginie Hamm[a], Christophe Kervévan[a], Dominique Thiéry[a], Louis de Lary[a], Jean-Charles Manceau[a]

[a]*BRGM, 3 av. Claude Guillemin, BP36009, 45060 Orléans CEDEX 2, France*

Abstract

This project aims at assessing the feasibility of the CO_2-DISSOLVED concept, combining injection of dissolved CO_2 and recovery of the geothermal heat. The objective here was to identify and to quantify the thermo-hydro-geochemical processes induced by a massive injection of dissolved CO_2 into a carbonated aquifer and a clastic reservoir. For that purpose, several simulations were performed using the MARTHE-PHREEQC and MARTHE-REACT reactive transport codes. Simulation results corroborate the expected great reactivity of the carbonated reservoir under the injection of CO_2-rich brine. Numerical results provide new arguments confirming the feasibility of the CO_2-DISSOLVED approach.

Peer-review under responsibility of the organizing committee of GHGT-13.

Keywords: MARTHE ; PHREEQC ; REACT ; CO_2-dissolved

1. Introduction

This research was conducted in the framework of the CO_2-DISSOLVED project [1] co-funded by the ANR (French National Research Agency). This project aims at assessing the feasibility of a novel CO_2 injection strategy in deep saline aquifers, combining injection of dissolved CO_2 (rather than supercritical CO_2) and recovery of the geothermal heat from the extracted brine [2]. This approach relies on the geothermal doublet technology, where the warm water is extracted at a production well and re-injected as cooled water, after heat extraction, in the same aquifer *via* a second well (injection well). The CO_2-DISSOLVED project combines several objectives including

* Corresponding author. Tel.: +3-323-864-3343; fax: +3-323-864-3062.
E-mail address: n.marty@brgm.fr

Peer-review under responsibility of the organizing committee of GHGT-13.
doi:10.1016/j.egypro.2017.03.1547

renewable energy production, greenhouse gas reduction, and the assessment of a novel, low-cost capture and storage method. Further, the proposed use of dissolved CO_2 versus injection in a supercritical phase offers substantial benefits in terms of lower brine displacement risks, lower CO_2 escape risks, and the potential for more rapid mineralization.

The objective of the work presented here was to identify and to quantify the Thermo-Hydro-geoChemical (THC) processes induced by a massive injection of dissolved CO_2 into (1) a carbonated aquifer (Dogger of the Paris basin - 1,500 to 2,000 m deep - 70°C) and (2) a clastic reservoir (Triassic sandstones of the Paris basin - 2,000 to 2,500 m deep - 90°C), and to evaluate their possible consequences on the feasibility of the CO_2-DISSOLVED concept. The space scale investigated ranged from the near-well zone area (a few meters) to the site scale (a few kilometers). A 30 years CO_2 injection period was simulated (operational lifetime of the geothermal doublet commonly met in the Paris basin). Though generic cases, both carbonated and clastic reservoirs were tested. For that purpose, several simulations were performed with MARTHE-REACT[3, 4] and MARTHE-PHREEQC[5, 6], see http://marthe.brgm.fr/.

Nomenclature

r	dissolution/precipitation rates (mol s^{-1} kg^{-1}_w)
m	subscript referring to the mineral under consideration
k	dissolution constant (mol m^{-2} s^{-1})
A	reactive surface area (m^2 kg^{-1}_w)
Ω	saturation ratio
θ	power term determined experimentally in order to describe the rate dependency on the saturation ratio
η	power term determined experimentally in order to describe the rate dependency on the saturation ratio
T	temperature (K)
k_{25}	dissolution constant at 25 °C (mol m^{-2} s^{-1})
E_a	activation energy (J mol^{-1})
R	ideal gas constant (8.314 J mol^{-1} K^{-1})
nu	superscript referring to reaction under neutral pH conditions
i	superscript referring to reaction under other pH conditions
a	activity of species
j	species index involved in one mechanism
n	power term

2. Thermodynamic database and kinetic parameters

2.1. THERMODDEM

The THERMODDEM thermodynamic database [7] (http://thermoddem.brgm.fr/) was used for the simulations performed on the clastic and carbonated reservoirs. This database is available in different formats: PHREEQC, TOUGHREACT, CRUNCH, Geochemical workbench and CHESS (geochemical module used by HYTEC).

2.2. Reaction rates and kinetic parameters

It is widely known that mineral dissolution rates depend on several kinetic parameters. Generally, the effects that physical and chemical parameters exert on mineral weathering rates (temperature, pH, catalysis/inhibition by aqueous species and solution saturation state) are incorporated in a general form of mineral dissolution. TST (Transition State Theory) kinetic laws are included in most geochemical codes. Dissolution/precipitation rates of a mineral (m) at different pH values and constant temperature are given by [8, 9]:

$$r_m = \pm k_m A_m \left| 1 - \Omega_m^{\theta} \right|^{\eta} \quad (1)$$

Note that parameters θ and η must be determined experimentally in order to describe the rate dependency on the saturation ratio. However, these parameters are only rarely found for mineral dissolution, because reactions are usually studied far from equilibrium.

The dissolution constant (k in the above equation) is expressed as [4, 10]:

$$k = k_{25}^{nu} \exp\left[\frac{-E_a^{nu}}{R} \left(\frac{1}{T} - \frac{1}{298.15} \right) \right] + \sum_i k_{25}^{i} \exp\left[\frac{-E_a^{i}}{R} \left(\frac{1}{T} - \frac{1}{298.15} \right) \right] \prod_j a_{ij}^{n_{ij}} \quad (2)$$

Whatever the considered case (carbonated or clastic reservoirs), dissolution/precipitation reactions of primary phases were controlled by kinetic laws. The kinetic parameters were extracted from a literature review [11]. The precipitation of secondary minerals was processed at local equilibrium. Their resulting precipitation rates are controlled by evolution of the activities of aqueous species in pore water provided by the dissolution of the primary phases (kinetically controlled) and mass transport.

3. Input parameters and modelling assumptions

The parameters used for the simulations were defined using the data available in the literature and are summarized in table 1.

Table 1. Parameters used for the simulations.

Parameters	Triassic sandstone	Carbonated limestone	Units
Depth (hanging wall)	2,500	1,500	m
Productive thickness	25	20	m
Reservoir pressure	250	150	kg cm^{-2}
Reservoir temperature	90	70	°C
Porosity	15	15	%
Specific storage	10^{-6}	10^{-6}	m^{-1}
Intrinsic permeability	130	2000	mD
Fluid salinity	30	15	g l^{-1}
Fluid heat conductivity	0.6	0.6	W m^{-1} °C^{-1}
Fluid heat capacity	4.18	4.18	MJ m^{-3} °C^{-1}
Rock heat conductivity	2.5	2.5	W m^{-1} °C^{-1}
Rock heat capacity	2.2	2.3	MJ m^{-3} °C^{-1}

Two mineralogical assemblages were assumed as representative for the carbonated and clastic reservoirs (table 2). In both cases a porosity of 15 % was considered.

Table 2. Mineralogical compositions considered for the modelling of the carbonated and clastic reservoirs (assuming a porosity of 15 %).

Reservoir	Minerals	Chemical formula	Volume fraction (%)	mol L^{-1} of medium
Carbonated limestone	Calcite	$CaCO_3$	0.95	21.87
	Disordered dolomite	$CaMg(CO_3)_2$	0.025	0.33
	Quartz	SiO_2	0.025	0.94
Triassic sandstone	K-fledspar (microcline)	$KAlSi_3O_8$	0.1	0.78
	Disordered dolomite	$CaMg(CO_3)_2$	0.05	0.66
	Quartz	SiO_2	0.85	31.84

Equilibrated pore waters with respect to carbonated and clastic reservoirs are reported in table 3. The pore water of the carbonated limestone was calculated used PHREEQC considering a low salinity of the aquifer (i.e. NaCl = 5

10^{-4} M); the solution chemistry is characteristic of Dogger pore water extracted from Coulommiers well (see [12] for more details). In contrast, the ionic strength of the pore water of the Triassic sandstone was assumed to be higher (i.e. NaCl 5 10^{-1} M). Note that the ionic strength of the Triassic pore water was about 0.5 and therefore, the extended Debye-Hückel activity model remains valid.

Table 3. Chemical compositions of the carbonated and clastic pore waters (PHREEQC calculations).

	Carbonated limestone	**Triassic sandstone**
Elements	Chemical composition at 70 °C (mol kg^{-1}_w)	Chemical composition at 90 °C (mol kg^{-1}_w)
C(4)	6.00 10^{-03}	1.13 10^{-02}
Al	--	2.03 10^{-07}
Ca	1.01 10^{-03}	1.71 10^{-03}
Cl	5.00 10^{-04}	5.00 10^{-01}
Mg	1.28 10^{-03}	1.71 10^{-03}
Na	5.00 10^{-04}	5.00 10^{-01}
K	--	2.65 10^{-03}
Si	5.66 10^{-04}	8.33 10^{-04}
pH	6.75	6.67

The injected cooled down water composition is given in table 4. A CO_2 concentration of 1 M has been considered. The fluid is supposed in equilibrium at 40 °C with calcite, dolomite and quartz whatever the considered case (clastic or carbonated reservoirs). The resulting ionic strength was about 0.5.

Table 4. Chemical composition of the injected pore waters (PHREEQC calculation).

Elements	Chemical composition at 40 °C (mol kg^{-1}_w)
C(4)	1.01
Ca	1.01 10^{-03}
Cl	1.00 10^{-03}
Mg	1.28 10^{-03}
Na	1.00 10^{-03}
Si	5.66 10^{-04}
pH	3.93

4. Coupled THC simulations performed at the injection well scale

4.1. Conceptual model

A 2D radial geometry was considered to finely investigate the phenomena involved around the injection well without being high CPU time consuming (< 1 day). Model was developed with this 2D geometry to be representative of each reservoir studied. Note that, for clarity reasons, only modelling dealing with the carbonated reservoir are presented in this section. Coupled THC simulations of the clastic reservoir are tackled in section 5. Carbonated reservoir was approximated as a horizontal porous layer with homogeneous hydraulic, chemical and thermal properties. In order to take into account more accurately the heat exchange processes, the reservoir was assumed to be surrounded by both an upper and a lower horizontal impermeable layers of known thermal properties (Fig. 1). The models thus account for thermal, hydraulic and chemical processes involved during the CO_2 injection.

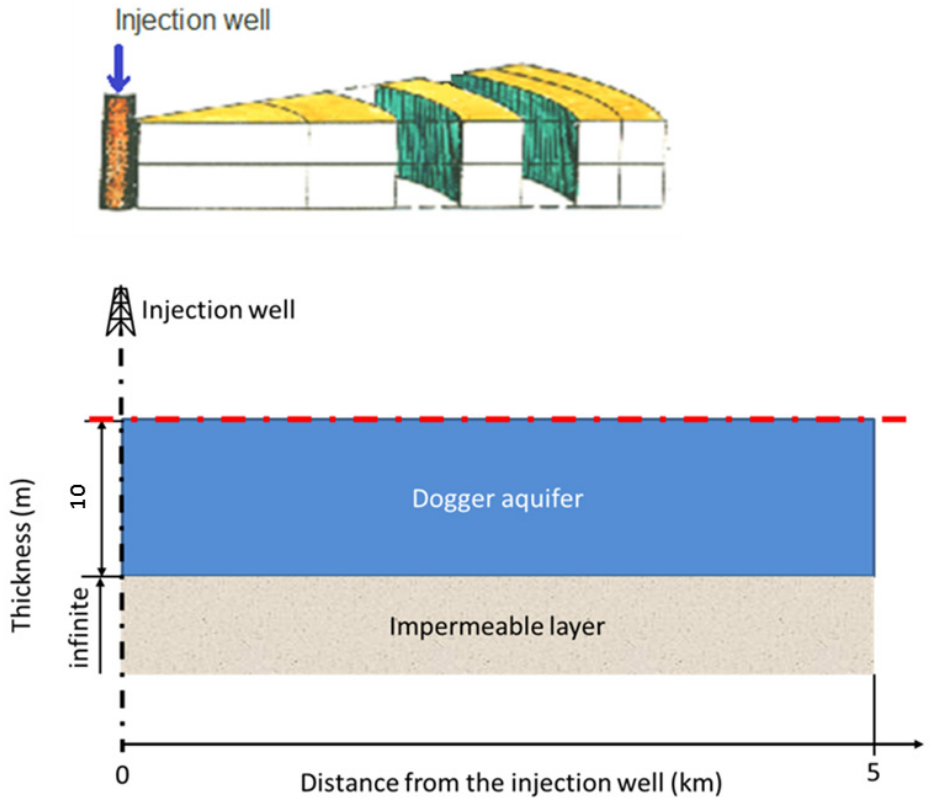

Fig. 1. Schematic representation of the 2D radial geometry used for the simulations performed at the injection well scale, in which axis of symmetry are represented by dashed curves. Figure modified from Castillo and co-workers [12].

4.2. Results obtained for the carbonated reservoir after 30 years of cooled and acidified water injection

Simulation was performed using with a time-step of 1 month/100. The results obtained with MARTHE-REACT and MARTHE-PHREEQC are reported in the Fig. 2.

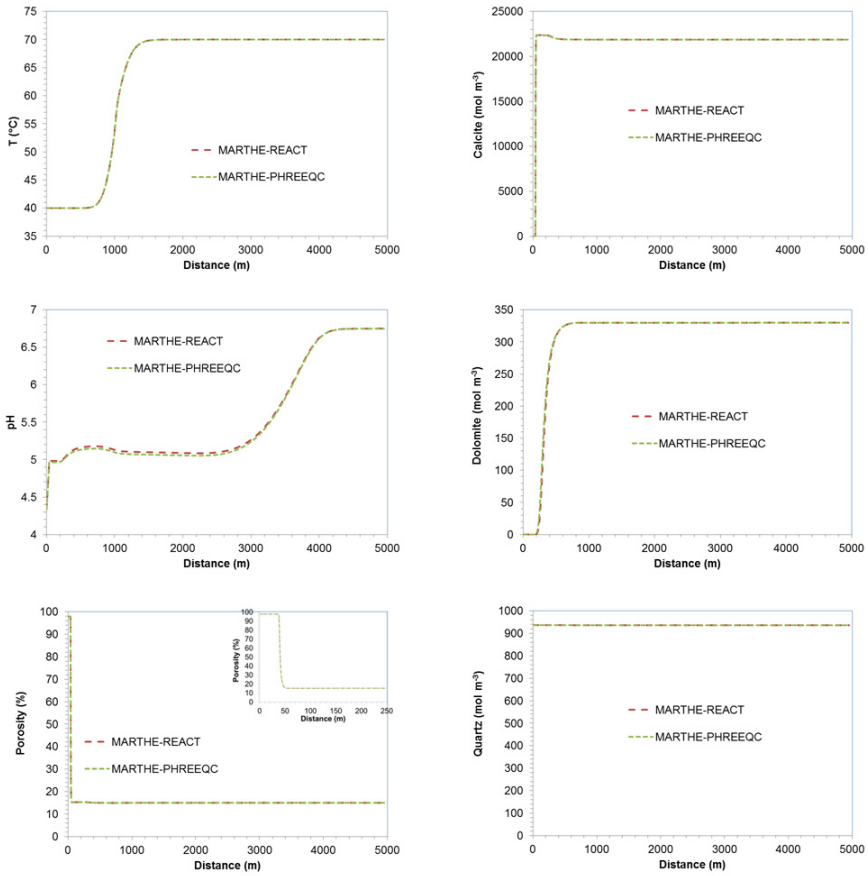

Fig. 2. Comparison of the results obtained with MARTHE-REACT and MARTHE-PHREEQC. Temperature, pH, calcite, dolomite, quartz and porosity x-profiles after 30 years of cooled and acidified water injection.

Numerical results after 30 years of cooled and acidified water injection showed:

- a decrease of the water temperature (up to 40°C) in the first 500 meters around the injection well;
- a strong acidification of the pore-water (up to 4.3) in the near field of the injection well;
- an increase of porosity (up to 97.5%) in the near-injection well area (up to 30 meters) due to the massive dissolution of carbonates (calcite and dolomite). In details, calcite and dolomite present, respectively, in the first 30 and 300 meters around the injection well are totally dissolved after 30 years of water injection;
- an insignificant quartz dissolution around the injection well.

Thus, it appeared that the geothermal exploitation of the Dogger reservoir (in place since the early 70's in the Paris basin) induces geochemical reactions that can already have an impact on porosity.

Results obtained with MARTHE-REACT and MARTHE-PHREEQC are very similar demonstrating the robustness of the codes. Slight differences could be attributed to ionic activity models. PHREEQC considers hydrated radius a_0 parameters for the extended Debye-Hückel activity-composition model. REACT uses a different version of the extended Debye-Hückel model, after Helgeson and co-workers [13]. Moreover, the two codes do not use the same polynomial equation for the temperature dependence of equilibrium-constant calculations.

5. Coupled THC simulations performed at the doublet scale

5.1. Conceptual model

As MARTHE-REACT and MARTHE-PHREEQC gave similar results (see section 4.2), only results obtained with MARTHE-PHREEQC are illustrated in this paragraph for clarity reasons. A pseudo-3D multilayer geometry focused on the doublet area was considered to simulate the injection at the well scale (Fig. 3).

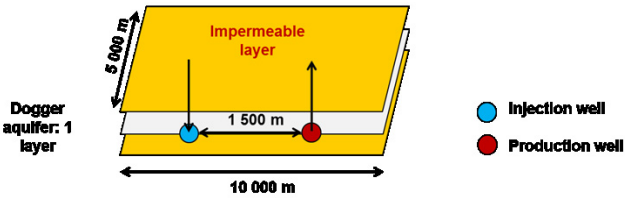

Fig. 3. Geometry considered for the simulations of reactive transport simulations at the doublet scale (example of the carbonated reservoir).

Two models (one for carbonated limestone and another one for the Triassic sandstone) were developed with this pseudo-3D geometry to be representative of each of the reservoir studied. Both are based on homogeneous hydraulic, chemical and thermal properties. The horizontal dimensions of the domain are 10 x 5 km in x, y using a symmetry at y = 0. The domain is divided in rectangular cells of 100 x 100 m, with a horizontal refinement of 25 x 25 m in the vicinity of the wells. The layer thickness is 25 and 20 m, which is representative of the cumulated average thickness of the productive layers in the clastic and in the carbonated reservoirs, respectively. Heat conduction in base and cap-rock is solved in z direction using a semi-analytical solution developed by Vinsome and Westerfeld [14], included in MARTHE, added to the 3D numerical simulation of heat transport (conduction plus advection) in the reservoir layer. The symmetry used along the doublet axis allowed us to reduce the model meshing (147 056 cells) and benefits long-lasting simulations.

5.2. Results obtained for the carbonated reservoir after 30 years of cooled and acidified water injection

Simulation was performed using with a time-step of 1 month/10. The temperature profile calculated after 30 years of cooled-water injection is reported on Fig. 4a. The temperature profile is slightly asymmetrical due to the existence of a flux between the injection and the production wells (noted as i and p on Fig. 4). Even after 30 years of injection of cooled water, the temperature remains at 70 °C around the production well. Therefore, the design of the geothermal device appears to be efficient for the geothermal production.

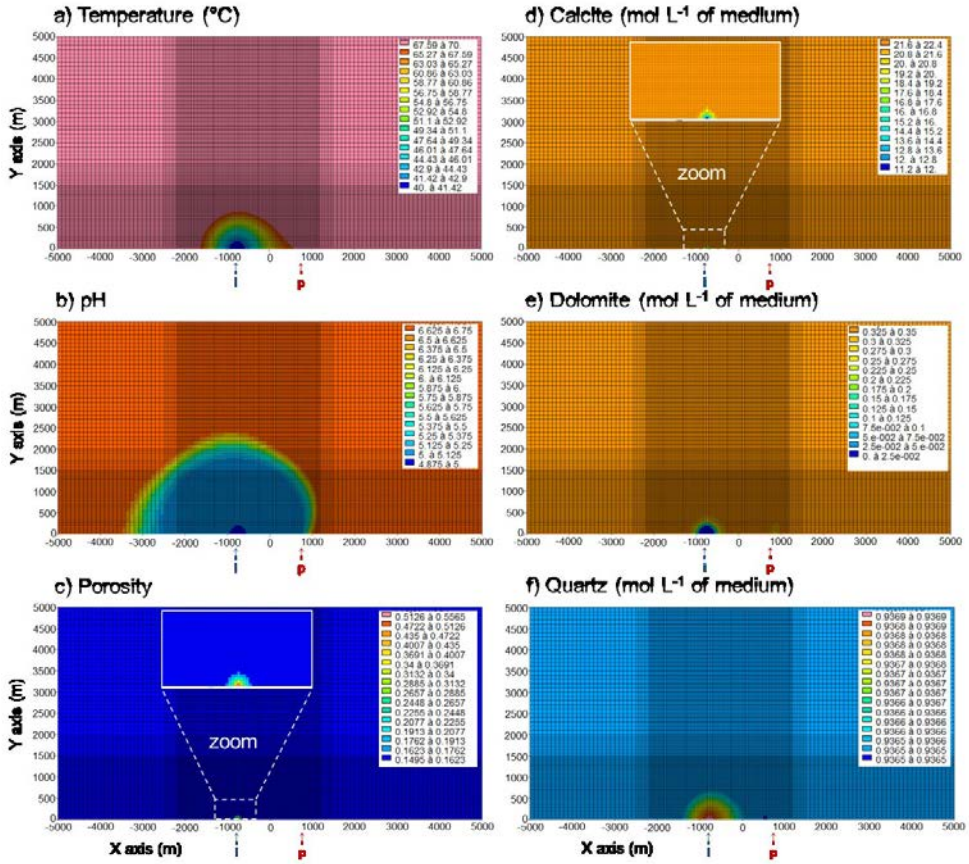

Fig. 4. Temperature (°C), pH, porosity, calcite (mol L^{-1} of medium), dolomite (mol L^{-1} of medium) and quartz (mol L^{-1} of medium) profiles in the carbonated reservoir after 30 years of cooled and acidified water injection (MARTHE-PHREEQC calculation). i and p stand for the injection (-750 m) and production (750 m) wells, respectively.

The pH profile obtained after 30 years of cooled-water injection is reported on Fig. 4b. As expected, the injection of a fluid saturated in CO_2 decreases the pH around the injection well.

Calcite, dolomite and quartz profiles (i.e. primary minerals) are reported on Fig. 4d, e and f, respectively. Calcite is partially altered in cells located around the injection well (40 % of calcite dissolution). In contrast, due to its weak content inside the Dogger formation (table 2), a total dissolution of dolomite is observed around the injection well (up to 200 m around the injection well after 30 years of cooled-water injection, see Fig. 4e). A carefully examination of numerical indicates a carbonate dissolution at the production well. This area is a mixing zone of two contrasted waters. The first one coming from the injection well contains about 1 M of dissolved CO_2 and is equilibrated at 70 °C with the Dogger mineralogy (i.e., with respect to calcite, dolomite and quartz). The second one is the pore water of the carbonated formation and therefore is also equilibrated at 70 °C with the primary minerals but is characterized by a weakest CO_2 content. Table 5 presents the saturation index (SI) of calcite, dolomite and quartz resulting from such mixing (simple batch calculations using PHREEQC and the THERMODDEM database). Results indicate that, even if these two waters are initially in equilibrium with carbonates, the resulting mixing is systematically under-saturated with respect to calcite and dolomite ($SI_{calcite} < 0$ and $SI_{dolomite} < 0$). Carbonates are therefore dissolved in the near field of the production well. In contrast, as the quartz solubility is constant for pH ranging from 0 to 8, the mineral remains in equilibrium ($SI_{quartz} = 0$).

Table 5. Saturation index (SI) of calcite, dolomite and quartz resulting from the mixing of two waters in equilibrium with respect these minerals but at various pCO2. Water 1: acidified water (1 M of CO_2) in equilibrium at 70 °C with respect to calcite, dolomite and quartz. Water 2: Dogger type water in equilibrium at 70 °C with respect to calcite, dolomite and quartz.

Water mixing	pH at 70 °C	$SI_{CO2(g)}$	$SI_{calcite}$	$SI_{dolomite}$	SI_{quartz}
100 % water 1	4.94	1.84	0.00	0.00	0.00
75 % water 1 25 % water 2	4.96	1.71	-0.14	-0.28	0.00
50 % water 1 50 % water 2	5.00	1.53	-0.34	-0.66	0.00
25 % water 1 75 % water 2	5.09	1.23	-0.63	-1.26	0.00
100 % water 2	6.75	-1.00	0.00	0.00	0.00

Due to its low solubility in acidic conditions, the amount of quartz remains almost constant even after 30 years of cooled-water injection (Fig. 4f). Note that color map has not been optimized and color variations are not significant. Hydromagnesite ($Mg_5(CO_3)_4(OH)_2{:}4H_2O$) has been considered as a potential secondary phase. The phase has been considered rather than magnesite (another Mg-carbonate); the latter is formed at temperatures higher than 60-80 °C (see [15] for a detailed discussion). However, numerical results indicate that the hydromagnesite formation is unlikely in our conditions (pH, temperature etc.). The porosity evolution resulting from mineralogical modification is reported on Fig. 4c. An increase of porosity up to 50 % is observed at the injection well due to carbonates dissolutions (i.e. calcite and dolomite alterations).

Another key point concerns the localization of the bubble point that could possibly be reached within the aquifer at the vicinity of the depressurized area around the production well [16, 17]. Of course, the possible apparition of a gas phase has to be avoided for obvious safety reasons (this will be part of the sensitivity analysis performed in this subtask). Multiphase transport modeling with dissolution cannot be performed with MARTHE. Nevertheless, the (P,T,salinity) conditions and C(4) concentrations (Fig. 5) encountered in the reservoirs and the related CO_2 solubility were closely examined. The CO_2 gas formation appears to be unlikely.

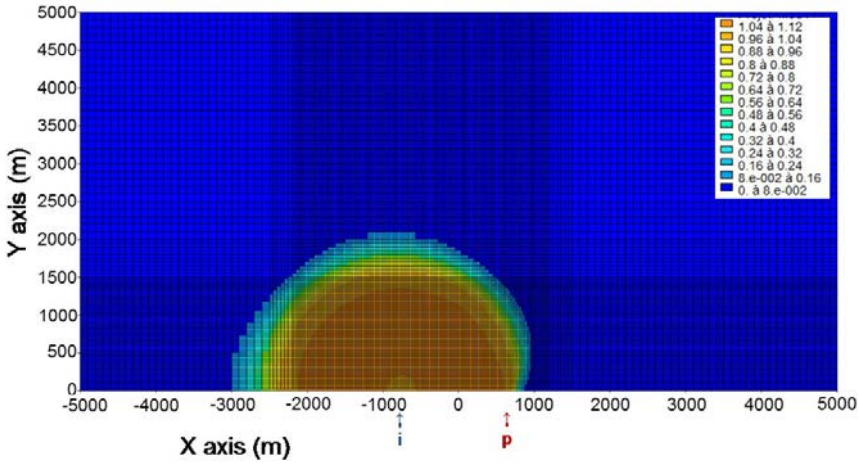

Fig. 5. C(4) concentration profile (mol L^{-1}) in the carbonated reservoir after 30 years of cooled and acidified water injection (MARTHE-PHREEQC calculation). i and p stand for the injection (-750 m) and production (750 m) wells, respectively.

5.3. Results obtained for the clastic reservoir after 30 years of cooled and acidified water injection

Simulation was performed using with a time-step of 1 month/10. The temperature profile simulated after 30 years of cooled and acidified water injection inside the Triassic formation is reported on Fig. 6a. The temperature remains at a constant value of 90 °C at the production well. Therefore, the design of the geothermal device applied to the

clastic reservoir is also efficient. The distance between the production and the injection well (2,500 m) could be twice reduced considering an operating period of 30 years.

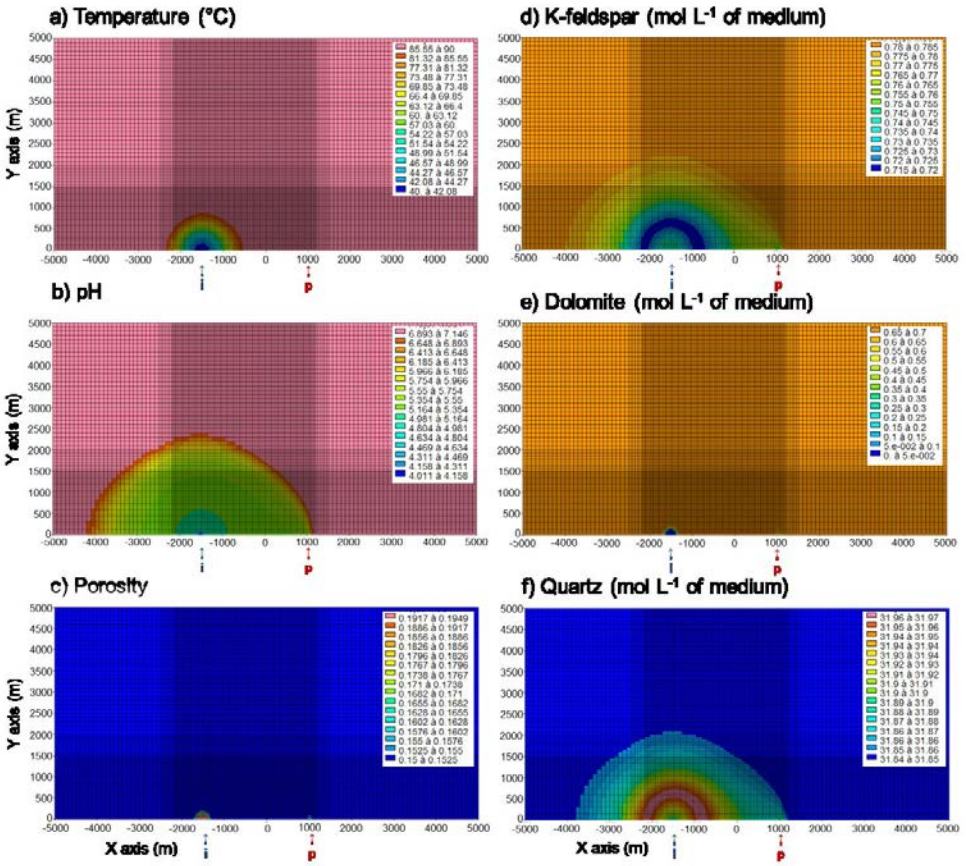

Fig. 6. Temperature (°C), pH, porosity, dolomite (mol L^{-1} of medium), K-fledspar (mol L^{-1} of medium) and quartz (mol L^{-1} of medium) profiles in the clastic reservoir after 30 years of cooled and acidified water injection (MARTHE-PHREEQC calculation). i and p stand for the injection (-1,500 m) and production (1,000 m) wells, respectively.

The pH profile obtained after 30 years of cooled and acidified water injection inside the Trias formation has been reported on Fig. 6b. Again, as expected, the injection of CO_2-rich water (table 4) decreases the pH around the injection well. Nonetheless, the pH perturbation presents a greater extends than the one observed in the case of a carbonated limestone.

K-felspar and quartz (Fig. 6d), the main minerals of the clastic reservoir (table 3), appears to be weakly altered even after 30 years of cooled and acidified water injection. Note that color maps have not been optimized and variations are almost insignificants. The dolomite profile is reported on Fig. 6e. The carbonate appears to be totally dissolved around the injection well. Due to a mixing between the Triassic pore water and the injected fluid, a weak dissolution is also observed at the production well. As shown on Fig. 6c, carbonate dissolution increases the porosity in both the area around the injection and the production wells. Note that due to the weak dolomite content inside the clasti reservoir, the porosity change remains limited (i.e. < 0.2).

Illite, kaolinite, gibbsite and hydromagnesite were considered as potential secondary minerals. Numerical results indicate that gibbsite and hydromagnesite precipitations are unlikely. In contrast, illite and kaolinate may precipitate from released elements due to the weak quartz and K-felspar alterations (Fig. 7). Note that the kaolinite formation is

possible under acidic conditions. Indeed Yang and Steefel [18] have been studied kaolinite formation at pH 4 and low temperature (i.e. 22 °C). In contrast, modelling results indicate the precipitation of illite at pH > 5.

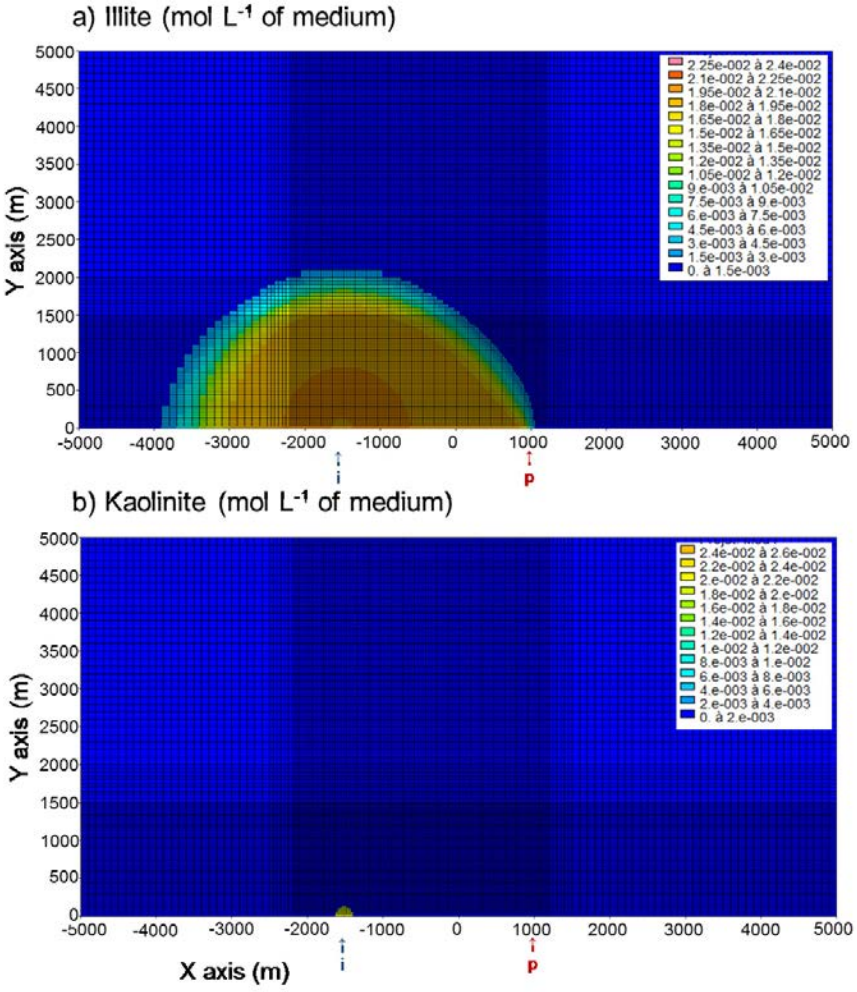

Fig. 7. Illite and kaolinite (mol L^{-1} of medium) profiles in the clastic reservoir after 30 years of cooled and acidified water injection (MARTHE-PHREEQC calculation). i and p stand for the injection (-1,500 m) and production (1,000 m) wells, respectively.

6. Conclusions

The results obtained with MARTHE-PHREEQC and MARTHE-REACT are very similar demonstrating then the robustness of the codes. In regards to the geothermal production, whatever the reservoir considered, it appears that the continuous injection of cooled down and acidified formation water (1 M of CO_2) does not cause a decline of the production temperature. The design of the geothermal device is *a priori* efficient. Nevertheless, it induces a strong acidification of the pore-water. The pH decline is particularly significant for the clastic reservoir, because the buffer capacity of its mineral is less important than those of the carbonated reservoir.

It appears that the continuous injection of dissolved CO_2 during 30 years induces a massive dissolution of carbonates (calcite and/or dolomite) around the injection wells. Carbonate alteration impacts the porosity. The porosity of the carbonated reservoir is significantly enhanced around the injection well and slightly increased around the production well after 30 years of injection. However, despite this reactivity, risk assessment study show

negligible effects due to dissolution on surface subsidence and horizontal surface strain due to the great depth of the reservoir [19]. Regarding the clastic reservoir, the porosity increases slightly around the injection and production wells. Nonetheless, the impact on the porosity is lower for the clastic reservoir than for the carbonate due to its weaker carbonate content (5% against 97.5% for the carbonated aquifer). All the simulation results corroborate the expected great reactivity of the carbonated reservoir under the injection of CO_2-rich brine that was observed experimentally [20].

Moreover, it can be observed that the injection of dissolved CO_2 into the clastic reservoir could also induce a very slight dissolution of quartz and K-feldspar initially present in the reservoir. Illite and kaolinite, considered as secondary phases, precipitated. Nonetheless, taking into account precipitated volumes, these reactions do not impact the porosity of the reservoir. As any C(4) bearing phases precipitate, the injected CO_2 remains stored in the aqueous phase. Therefore, CO_2 reactivity does not have a significant impact on the CO_2 mass balance at the site scale when compared with the non-reactive simulations carried out previously by Hamm and co-workers [21].

Acknowledgements

We would like to thank the ANR (French National Research Agency) and the BRGM for co-funding this study in the framework of the CO_2-DISSOLVED project.

References

[1] C. Kervévan, M.H. Beddelem, K. O'Neil, CO_2-DISSOLVED: a Novel Concept Coupling Geological Storage of Dissolved CO_2 and Geothermal Heat Recovery – Part 1: Assessment of the Integration of an Innovative Low-cost, Water- based CO_2 Capture Technology, Energy Procedia, 63 (2014) 4508-4518.

[2] C. Castillo, S. Knopf, C. Kervévan, F. May, CO_2-DISSOLVED: a Novel Concept Coupling Geological Storage of Dissolved CO_2 and Geothermal Heat Recovery – Part 2: Assessment of the Potential Industrial Applicability in France, Germany, and the U.S.A, Energy Procedia, 63 (2014) 4519-4535.

[3] D. Thiéry, N. Jacquemet, G. Picot-Colbeaux, C. Kervévan, L. André, M. Azaroual, Validation of MARTHE-REACT coupled surface and groundwater reactive transport code for modeling hydro systems, in: TOUGH Symposium 2009, Berkeley (California), United States, 2009, pp. pp. 576-583.

[4] T. Xu, E. Sonnenthal, N. Spycher, K. Pruess, TOUGHREACT-A simulation program for non-isothermal multiphase reactive geochemical transport in variably saturated geologic media: Applications to geothermal injectivity and CO2 geological sequestration, Computers & Geosciences, 32 (2006) 145-165.

[5] D. Thiéry, Modélisation 3D du Transport Réactif avec le code de calcul MARTHE v7.5 couplé aux modules géochimiques de PHREEQC, in: R. BRGM/RP-65010-FR (Ed.), Orléans, France, 2015, pp. 164, available at http://infoterre.brgm.fr/rapports/RP-65010-FR.pdf .

[6] D.L. Parkhurst, C.A.J. Appelo, Description of input and examples for PHREEQC version 3 - A computer program for speciation, batch-reaction, one-dimensional transport, and inverse geochemical calculations, in, U.S. Geological Survey Techniques and Methods, , book 6, chap. A43, 497 p., available only at http://pubs.usgs.gov/tm/06/a43. , 2013.

[7] P. Blanc, A. Lassin, P. Piantone, M. Azaroual, N. Jacquemet, A. Fabbri, E.C. Gaucher, Thermoddem: A geochemical database focused on low temperature water/rock interactions and waste materials, Applied Geochemistry, 27 (2012) 2107-2116.

[8] A.C. Lasaga, Transition state theory, Reviews in Mineralogy and Geochemistry, 8 (1981) 135-168.

[9] A.C. Lasaga, J.M. Soler, J. Ganor, T.E. Burch, K.L. Nagy, Chemical weathering rate laws and global geochemical cycles, Geochimica et Cosmochimica Acta, 58 (1994) 2361-2386.

[10] T. Xu, N. Spycher, E. Sonnenthal, G. Zhang, L. Zheng, K. Pruess, TOUGHREACT Version 2.0: A simulator for subsurface reactive transport under non-isothermal multiphase flow conditions, Computers & Geosciences, 37 (2011) 763-774.

[11] N.C.M. Marty, F. Claret, A. Lassin, J. Tremosa, P. Blanc, B. Madé, E. Giffaut, B. Cochepin, C. Tournassat, A database of dissolution and precipitation rates for clay-rocks minerals, Applied Geochemistry, 55 (2015) 108-118.

[12] C. Castillo, C. Kervévan, D. Thiéry, Geochemical and reactive transport modeling of the injection of cooled Triassic brines into the Dogger aquifer (Paris basin, France), Geothermics, 53 (2015) 446-463.

[13] H.C. Helgeson, D.H. Kirkham, G.C. Flowers, Theoretical prediction of the thermodynamic behavior of aqueous electrolytes by high pressures and temperatures; IV, Calculation of activity coefficients, osmotic coefficients, and apparent molal and standard and relative partial molal properties to 600 degrees C and 5kb, American Journal of Science, 281 (1981) 1249-1516.

[14] P.K.W. Vinsome, J. Westerveld, A Simple Method For Predicting Cap And Base Rock Heat Losses In' Thermal Reservoir Simulators.

[15] Q. Gautier, P. Bénézeth, V. Mavromatis, J. Schott, Hydromagnesite solubility product and growth kinetics in aqueous solution from 25 to 75 °C, Geochimica et Cosmochimica Acta, 138 (2014) 1-20.

[16] L. Jain, S.L. Bryant, Optimal design of injection/extraction wells for the surface dissolution CO_2 storage strategy, Energy Procedia, 4 (2011) 4299-4306.

[17] L. Jain, S.L. Bryant, Time weighted storage capacity for geological sequestration, Energy Procedia, 4 (2011) 4873-4880.

[18] L. Yang, C.I. Steefel, Kaolinite dissolution and precipitation kinetics at 22 °C and pH 4, Geochimica et Cosmochimica Acta, 72 (2008) 99-116.
[19] L. De Lary, J.-C. Manceau, A. Loschetter, J. Rohmer, O. Bouc, I. Gravaud, C. Chiaberge, P. Willaume, T. Yalamas, Quantitative risk assessment in the early stages of a CO_2 geological storage project: implementation of a practical approach in an uncertain context, Greenhouse Gases: Science and Technology, 5 (2015) 50-63.
[20] A. Randi, J. Sterpenich, C. Morlot, J. Pironon, C. Kervévan, M.H. Beddelem, C. Fléhoc, CO2-DISSOLVED: a Novel Concept Coupling Geological Storage of Dissolved CO_2 and Geothermal Heat Recovery – Part 3: Design of the MIRAGES-2 Experimental Device Dedicated to the Study of the Geochemical Water-Rock Interactions Triggered by CO_2 Laden Brine Injection, Energy Procedia, 63 (2014) 4536-4547.
[21] V. Hamm, C. Kervévan, D. Thiéry, CO_2-DISSOLVED: a Novel Concept Coupling Geological Storage of Dissolved CO_2 and Geothermal Heat Recovery – Part 4: Preliminary Thermo-Hydrodynamic Simulations to Assess the CO_2 Storage Efficiency, Energy Procedia, 63 (2014) 4548-4560.